

SCIENTIFIC REPORTS



OPEN

Promising Nanocarriers for PEDF Gene Targeting Delivery to Cervical Cancer Cells Mediated by the Over-expressing FR α

Received: 13 April 2016
Accepted: 09 August 2016
Published: 31 August 2016

Yuhan Yang^{1,*}, Lili He^{1,2,*}, Yongmei Liu^{1,*}, Shan Xia³, Aiping Fang¹, Yafei Xie¹, Li Gan¹, Zhiyao He¹, Xiaoyue Tan⁴, Chunling Jiang¹, Aiping Tong¹ & Xiangrong Song¹

Cervical cancer presents extremely low PEDF expression which is associated with tumor progression and poor prognosis. In this study, folate receptor α (FR α)-targeted nano-liposomes (FLP) were designed to enhance the anti-tumor effect by targeting delivery of exogenous PEDF gene to cervical cancer cells. The targeting molecule F-PEG-Chol was firstly synthesized by a novel simpler method. FLP encapsulating PEDF gene (FLP/PEDF) with a typical lipid-membrane structure were prepared by a film dispersion method. The transfection experiment found FLP could effectively transfect human cervical cancer cells (HeLa cells). FLP/PEDF significantly inhibited the growth of HeLa cells and human umbilical vein endothelial cells (HUVEC cells) and suppressed adhesion, invasion and migration of HeLa cells *in vitro*. In the abdominal metastatic tumor model of cervical cancer, FLP/PEDF administered by intraperitoneal injection exhibited a superior anti-tumor effect probably due to the up-regulated PEDF. FLP/PEDF could not only sharply reduce the microvessel density but also dramatically inhibit proliferation and markedly induce apoptosis of tumor cells *in vivo*. Moreover, the preliminary safety investigation revealed that FLP/PEDF had no obvious toxicity. These results clearly showed that FLP were desired carriers for PEDF gene and FLP/PEDF might represent a potential novel strategy for gene therapy of cervical cancer.

Cervical cancer, also called invasive cervical carcinoma, is the second malignant tumor to women all over the world¹. The early cervical cancer is absent of symptoms and could be curable by surgical intervention, radiation treatment and chemotherapy², among which radiation treatment and chemotherapy could produce serious side effect harming normal tissues. Moreover, the advanced and/or metastatic or recurrent tumors are the deadly ones to those patients with poor prognosis and less than 5% of them could be alive at 5 years³. Fortunately, gene therapy-based therapeutics in clinical trials, including growth factors, tumor suppressors, antigens, receptors and others⁴, have offered many exciting possibilities for treating cervical cancer.

Pigment epithelium-derived factor (PEDF) is an endogenous 50 kDa glycoprotein disseminating throughout the body⁵, which has been proved to present not only direct anti-tumor properties of apoptosis⁶, differentiation and anti-proliferation⁷ of tumor cells but also indirect characters like anti-angiogenesis⁸ possibly through vascular endothelial growth factor (VEGF) and inducing apoptosis of endothelial cells. Actually, PEDF has been reported to be as an anti-cancer agent against a range of tumors such as lung, breast, prostate, and ovary^{9–13}, but rarely in cervix. PEDF gene therapy might be a more promising therapeutic strategy in contrast to PEDF itself owing to more lasting curative effect, easier scale-up production and lower cost. PEDF gene indeed had better therapeutic efficacy on many tumors such as melanoma, hepatocellular carcinoma and colon carcinoma^{14–16}. Nevertheless,

¹State Key Laboratory of Biotherapy and Cancer Center, West China Hospital, Sichuan University, and Collaborative Innovation Center for Biotherapy, Sichuan University, Chengdu 610041, China. ²College of Pharmacy, Southwest University for Nationalities, Chengdu 610041, China. ³Chemistry and Life Science College, Chengdu Normal University, Chengdu 611130, China. ⁴Department of Pathology/Collaborative Innovation Center of Biotherapy, Medical School of Nankai University, Tianjin 300071, China. *These authors contributed equally to this work. Correspondence and requests for materials should be addressed to C.J. (email: jiang_chunling@yahoo.com) or A.T. (email: aipingtong@scu.edu.cn) or X.S. (email: songxr@scu.edu.cn)

there was still no report about PEDF gene therapy for cervix cancer, probably lacking a specific and efficient delivery carrier.

We previously developed a series of nanocarriers for PEDF gene delivery based on PLGA nanoparticles, which had achieved better *in vivo* therapeutic efficacy for colon carcinoma^{17,18}. However, these vectors had no active selectivity for cervix cancer cells. Cervical tumor tissues over-express folate receptor α (FR α) especially in metastatic focus and recurrent tumors¹⁹, which could provide conditions for folate-mediated targeting delivery for PEDF gene. Folate-decorated nanoparticles have been reported to successfully targeting deliver low molecular weight chemotherapeutic agents²⁰ or theranostic agents²¹ to cervix cancer tissues *in vivo*. Our group formerly constructed a novel non-viral gene vector, folate-modified nano-liposomes (FLP) which could specifically deliver therapeutic gene CLDN3 shRNA to ovarian cancer cells and thereby achieve high *in vivo* anti-tumor efficacy by recognizing the up-regulated FR α ²². Therefore, we hypothesized that FLP might also be suitable nano-carriers for efficient delivery of PEDF gene to cervical tumor cells.

In the present study, we investigated whether FLP could be used as PEDF gene vectors to battle cervix cancer. The targeting molecule F-PEG-Chol was firstly synthesized and purified by a novel simpler method. FLP, prepared by a self-assembly process, were subsequently complexed with PEDF gene to form FR α -targeted nano-lipoplexes (FLP/PEDF). Finally, FLP/PEDF were injected intraperitoneally to treat the peritoneal metastasis of cervical cancer. To our knowledge, we show for the first time that FLP are highly effective in delivering PEDF gene for cervix cancer therapy.

Experimental Section

Materials. 1,2-dioleoyl-3-trimethylammonium-propane (DOTAP) was purchased from Avanti Polar Lipids Inc. (Alabaster, AL, USA). Cholesterol (Chol) was obtained from Chengdu Kelong Chemical Co. Ltd & ChengDu Kelong Chemical Reagent Company (Chengdu, China). Cholesterol succinic anhydride ester (Chol-suc) was synthesized as described previously²³. Poly (ethylene glycol) diamine (H₂N-PEG-NH₂) was provided by BioMatrik Inc. (Jiaxing, Zhejiang, China). MPEG-succinyl-Cholesterolconjugate (mPEG-Chol) was synthesized and purified by our research group^{24,25}. The plasmid green fluorescent protein (pGFP), PEDF plasmid PAAV₂-PEDF (PEDF gene) and null plasmid PAAV₂ were constructed according to our previous report¹⁶. Plasmid DNA (pDNA) was extracted according to the EndoFree Plasmid Purification Handbook (QIAGEN, Germany). DNA ladder and pre-stained protein ladder were provided by Fermentas (Thermo Fisher Scientific Inc., Waltham, MA, USA). All reagents were of analytical grade and were used without further purification except chloroform used to prepare nano-liposomes.

Synthesis and Characterization of F-PEG-Chol. The synthesis route of F-PEG-Chol was presented in Fig. 1. According to our previous report²⁶, F-PEG-Chol was synthesized through a simple two-step reaction. Briefly, Chol-suc and H₂N-PEG-NH₂ were used to prepare the intermediate H₂N-PEG-Chol which was subsequently reacted with folate to form F-PEG-Chol. In this study, the synthetic process parameters and the purified method of H₂N-PEG-Chol were further optimized. Specifically, the mixture containing Chol-suc, NHS and EDCI (1:4:2, molar ratio) in dichloromethane reacted to generate the activated ester, which was then dropped into H₂N-PEG-NH₂ (molar ratio to mixture was 1.2). The reaction mixture was stirred at room temperature and monitored at the same time. Once Chol-PEG-Chol was detected, the reaction was terminated. The reaction liquid was washed by 1 M HCl solution and then saturated NaHCO₃ solution. The organic layer was dried with Na₂SO₄ and then rotarily evaporated. The obtained crude product was re-dissolved with dichloromethane, followed by recrystallization in petroleum ether and then centrifuged to get white crystal. After washed by diethyl ether, the product H₂N-PEG-Chol was air-dried. ¹H-NMR spectra of H₂N-PEG-Chol, Chol-suc and H₂N-PEG-NH₂ in CDCl₃ were recorded on a Unity Inova-400 (400 MHz) (Varian Inc., Palo Alto, CA, USA) at room temperature.

Preparation and Characterization of FLP/PEDF. FLP were prepared by a film dispersion method as described previously²⁵. In detail, DOTAP, Chol, mPEG-Chol and F-PEG-Chol were dissolved in chloroform. The solution was rotarily evaporated to remove the solvent and then the make-up film was further dried under high vacuum for 4–6 h. The dry lipid film was hydrated in 5% glucose solution, and the obtained suspension of lipids were sonicated by a probe to form translucent liposome solution. Thereafter, the colloidal solution was sterilized through a Millipore 0.22 μ m filter membrane to obtain FLP and stored at 4 °C before used. This method was also used to construct non-targeted nano-liposomes (PLP) containing DOTAP, Chol and mPEG-Chol and normal nano-liposomes (LP) consisting of DOTAP and Chol.

FLP/PEDF were prepared by mixing FLP with PEDF gene. Briefly, 1 mg/mL FLP in 5% glucose solution was added to 1 mg/mL PEDF in TE buffer. The mixture was mixed slightly and quickly for 3 times. After incubating for 30 min at room temperature, FLP/PEDF was finally formed. FLP/PAAV₂ were produced by mixing FLP with PAAV₂ in the same procedure. PLP/PEDF and PLP/PAAV₂ were assembled by the same approach as FLP/PEDF and FLP/PAAV₂, respectively. The particle size and zeta-potential of FLP/PEDF were measured by Zetasizer NanoZS ZEN 3600 (Malvern Instruments, Ltd., Malvern, Worcestershire, UK). The morphological characteristic was examined by a transmission electron microscope (TEM, H-600, Hitachi, Ltd, Japan).

Agarose gel electrophoresis was used to test the gene loading capacity of FLP. The electrophoresis was proceeded on 1% (w/v) agarose gel (Invitrogen Corp., Carlsbad, USA) in pH 7.4 TAE buffer containing Golden View as nucleic acid stain. 10 μ L of FLP/PEDF mixed with 2 μ L of loading buffer (Thermo Fisher Scientific Inc, USA) were applied to agarose at a constant voltage of 130 V for 20 min at room temperature. The electrophoresis gel was visualized and digitally photographed by a gel documentation system (Gel Doc 1000, Bio-Rad Laboratories, Hercules, CA, USA).

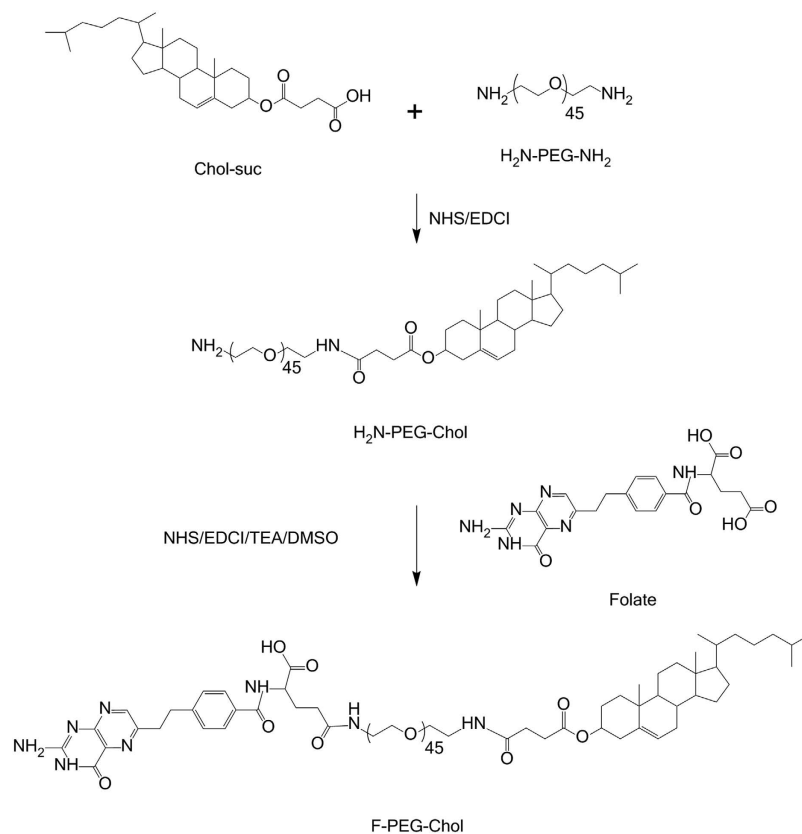


Figure 1. The synthesis route of F-PEG-Chol. F-PEG-Chol was synthesized through a simple two-step reaction. Specifically, Chol-suc and H₂N-PEG-NH₂ were used to prepare the intermediate H₂N-PEG-Chol which was subsequently reacted with folate to form F-PEG-Chol.

***In vitro* Anti-Tumor Activity Study.** *Cell Culture.* Human cervical cancer cells (HeLa cells) were obtained from the American Type Culture Collection. The cells were cultured as a monolayer in Roswell Park Memorial Institute-1640 Medium (RPMI1640, Gibco, Invitrogen Corp., Carlsbad, CA, USA) extra added with 10% calf serum, L-glutamine (2 mM), penicillin (100 U/mL) and streptomycin (100 µg/mL). Human umbilical vein endothelial cells (HUVEC cells) were obtained from the newborn's umbilical cord. The cells were cultured as a monolayer in Dulbecco's Modified Eagle's Medium (DMEM, Gibco, Invitrogen Corp., Carlsbad, CA, USA) supplemented with 10% fetal bovine serum and others were the same as above. They were both cultured in a humidified atmosphere containing 5% CO₂ at 37 °C.

Detection of FR α Expressed on HeLa cells. HeLa cells in culture dish were harvested after trypsinization with 0.25% EDTA and centrifuged, and the cells sediments were washed with PBS. They were divided into four groups as negative, second antibody, isotype control and positive group. 2 µL anti-hFOLR1 purified mouse monoclonal IgG1 (R&D Systems, Minneapolis, MN, USA) was added to the re-suspended cells in PBS in the isotype control and positive group. After incubation for 2 h at 4 °C, they were washed with PBS and then centrifuged, and finally resuspended with PBS. 2 µL anti-mouse IgG (Fc specific)-FITC (Sigma-Aldrich, St. Louis, MO, USA) was added to the second antibody group and positive group. After incubation for 30 min at 4 °C, the resuspended cell suspensions in PBS were analyzed by flow cytometer (BD Biosciences, San Jose, CA, USA) to determine the positive rate.

Transfection experiment. Transfection experiment was done as described previously²⁵. Lipo2000/GFP were prepared according to the protocol of Lipofectamine™ 2000 (Lipo2000). FLP/GFP, PLP/GFP and LP/GFP were formulated by mixing GFP with FLP, PLP and LP in the same approach as FLP/PEDE, respectively. HeLa cells were seeded on 6-well plates (Corning Inc., NY, USA) at 5 × 10⁴ cells per well in 2 mL RPMI1640 with 10% calf serum. After adherence for 24 h, the culture medium was replaced by 800 µL of folate free RPMI1640 (serum-free) in each well. The nano-lipoplexes (FLP/GFP, PLP/GFP, LP/GFP and Lipo2000/GFP) in a final volume of 200 µL containing 1 µg GFP gene were subsequently added to the wells. After 6 h of incubation, cell culture medium was changed to RPMI1640 with calf serum and the cells were incubated for extra 42 h. The expressed GFP was observed under an Olympus IX 71 inverted fluorescence microscope (Olympus Corp., Tokyo, Japan). Then the cells were harvested after trypsinization with 0.25% EDTA and centrifuged, and the cells sediments were washed with PBS. The re-suspended cell suspensions in PBS were analyzed by flow cytometer to determine the transfection efficiency.

Cytotoxicity assay of FLP/PEDF. Cytotoxicity of FLP/PEDF was carried out by MTT assay on HeLa cells and HUVEC cells as described previously²⁷. In brief, cells were planted into 96-well plates (Corning Inc., NY, USA) at a density of 3×10^3 cells per well in 100 μ L medium. After attaching overnight, cells were treated with another 100 μ L various concentrations of FLP/PEDF and further incubated for another 24 h, 48 h or 72 h to assess concentration-dependent and time-dependent cytotoxicity. At the end of predetermined time, 20 μ L MTT solution (5 mg/mL in saline) was added to each well and cells were further cultured at 37 °C for extra 4 h. Finally, the culture media were removed and then 150 μ L DMSO was added to each well to dissolve formazan crystals. The OD value of each well was read at 490 nm on a Multiskan MK3 microplate reader (Thermo Fisher Scientific Inc., Waltham, MA, USA). The parallel cytotoxicity experiment was performed on the contrast formulations including FLP/PAAV₂, PLP/PEDF, PLP/PAAV₂, FLP, PLP and Lipo2000 in parallel experiment. Untreated cells were used as controls. The relative cell viability compared to control was calculated as below:

$$\text{Relative cell viability (\%)} = \text{OD}_{\text{treated}} / \text{OD}_{\text{Control}} \times 100\%$$

In vitro Anti-metastasis Research. Adhesion assay. Adhesion assay was operated by MTT assay²⁸. HeLa cells were firstly transfected with PLP/PAAV₂, FLP/PAAV₂, PLP/PEDF and FLP/PEDF, respectively. Briefly, HeLa cells were seeded on 6-well plates at 3×10^5 cells per well in 2 mL RPMI1640 with 10% calf serum. After adherence for 24 h, the culture medium was replaced by 800 μ L of folate free RPMI1640 in each well. The nano-lipoplexes containing 5 μ g PEDF gene or PAAV₂ in 200 μ L folate free RPMI1640 were subsequently added to the wells. HeLa cells transfected with nano-lipoplexes were finally collected after co-culture for 48 h. The treated cells were used as the experimental groups while the non-transfected HeLa cells were the control group. All the cells were planted into the Matrigel-coated 96-well plate in triplicate. After attachment for the predetermined time (30 min, 60 min and 90 min), the plate was washed to remove the non-adherent cells. The amount of attached cells was then measured by MTT assay at 490-nm wavelength. The relative adhesive rate compared to control was calculated as below:

$$\text{Relative adhesive rate (\%)} = \text{OD}_{\text{treated}} / \text{OD}_{\text{Control}} \times 100\%$$

Invasion assay. The invasion ability was investigated by transwell assay²⁹. 200 μ L HeLa cells (2×10^5 /mL in serum free RPMI-1640) transfected with nano-lipoplexes (PLP/PAAV₂, FLP/PAAV₂, PLP/PEDF and FLP/PEDF) were placed on the top chamber of each transwell (8 μ m pore size, Corning, America) coated with 50 μ L diluted Matrigel (volume ratio to RPMI-1640 serum-free was 1:3). The bottom chamber was filled with 500 μ L RPMI1640 medium with 10% calf serum to act as the nutritional attractant. At the end of invasion for 24 h, non-migrated cells on the top surface of membrane were removed by cotton swabs and then washed with PBS. Migrated cells on the bottom surface of membrane were fixed, stained, and counted. The migrated cells were observed under an Olympus BX 53 fluorescence microscope (Olympus Corp., Tokyo, Japan). All the experiments were performed independently in triplicate.

Scratch assay. HeLa cells were firstly planted into 6-well plates. When cells spread to 80–90%, straight lines were drawn by a pipette tip on the bottom of plate. The cells were then washed with PBS to remove the non-adhered cells. The nano-lipoplexes mentioned above were added to transfect all the cells. After 48 h, the cell migration into the scratches was observed under Olympus IX 71 inverted fluorescence microscope. The migration distance ratio was calculated as below³⁰:

$$\text{Migration distance ratio (\%)} = (1 - \text{scratch distances (48 h)} / \text{scratch distances (0 h)}) \times 100\%$$

In vivo Anti-cancer Study. Animals. Female athymic nude mice (BALB/c-nude, SPF) were purchased from Vital River (Beijing, China). The mice were fed under SPF conditions. All studies were approved and supervised by the State Key Laboratory of Biotherapy Animal Care and Use Committee (Sichuan University, Chengdu, Sichuan, China) and conform to the Guide for the Care and Use of Laboratory Animals published by the US National Institutes of Health. The mice were used until they were 6 to 8 weeks old.

Heterotopic Tumor Growth Assay. Mice were injected intraperitoneally with 0.2 mL HeLa cells suspension (1×10^7 cells in serum free RPMI-1640) and randomly separated into five groups based on their body weights two days after inoculation. They were administered once every third day with the nano-lipoplexes containing plasmid DNA (5 μ g) in 200 μ L volume. Treatment continued until the mice of the control group became moribund (typically 4 to 6 weeks). At the time of sacrifice, tumor tissues, whole blood, ascitic fluid and organs of mice were harvested. The ascitic fluid volumes, tumor weights and numbers of nodules were recorded. The tumor specimens were divided into two portions: Parts of the tumors were immediately lysed by RIPA lysis buffer (Sigma-Aldrich, St. Louis, MO, USA) containing proteinase inhibitor cocktail (Sigma-Aldrich, St. Louis, MO, USA), centrifuged, and the supernatant was stored at -80 °C for western blot analysis. The rest tumor tissues were fixed with paraformaldehyde in PBS (pH 7.4) and then imbedded by paraffin for tissue sectioning.

Immunohistochemistry Staining. Labeled streptavidin-biotin method was used in immunohistochemistry (IHC). PEDF expression, Ki₆₇ antigen and microvessel density (MVD, CD31) were analyzed with human serpin F1/PEDF antibody (R&D, USA), rabbit anti-human Ki₆₇ antibody (AbcamPLC, Boston, MA, USA) and rabbit anti-human CD31 antibody (AbcamPLC, Boston, MA, USA). Briefly, 4–5 μ m sections were made from paraffin-embedded tumor tissue specimens of each group and subsequently deparaffinized by sequentially

washed with xylene (I and II), 100% ethanol, 95% ethanol, 85% ethanol, 75% ethanol and water. Endogenous peroxidase was blocked with 3% H₂O₂ kept in dark place at room temperature for 10 min. Antigen retrieval was done by heated in a pressure cooker in 10 mM sodium citrate buffer (pH 6.0). After washed with PBS, tissues were blocked with goat serum for 30 min at 37 °C then incubated with primary antibody overnight at 4 °C. After washed with PBS for three times, the secondary antibody conjugated to horse radish peroxidase (HRP) was added. HRP was detected with 3,3'-diaminobenzidine substrate (DAB Kit, ZSGB-Bio, Beijing, China) for 30 s or more, terminated by water and re-dyed with hematoxylin (Beyotime Institute of Biotechnology, Shanghai, China) for 30–60 s. 10 random fields at ×400 magnification were examined for each section.

TUNEL Assay. Apoptotic cells were detected on paraffin sections according to the protocol of terminal deoxynucleotidyl transferase-mediated nick-end labeling (TUNEL) staining. Briefly, the sections mentioned above were deparaffinized by the same process as IHC. After washed with 0.85% sodium chloride solution and PBS and fixed with paraformaldehyde, sections were incubated with proteinase K solution (20 μg/mL) and then rTDT buffer at 37 °C for 60 min in a dark place. The sections were observed under a fluorescence microscope and digitally photographed by the Olympus Application Suite (Olympus Corporation, Japan). Cells with dark green fluorescent staining were defined as TUNEL-positive cells while total number of cells were counted in 10 random fields at ×400 magnification. Percent apoptosis was determined as below:

$$\text{Apoptosis cells (\%)} = \text{TUNEL-positive ones/total cells} \times 100\%$$

Western Bolt Analysis. Total protein concentrations of tumor tissues lysates were measured through the Bradford protein assay reagent kit (Bio-Rad Laboratories, Hercules, CA, USA). The PEDF protein was separated by 10% SDS-PAGE under reducing conditions and then transferred to Millipore PVDF membranes. Membranes were blocked with 5% skimmed milk and incubated with anti-PEDF antibody (R&D Systems, Minneapolis, MN, USA) at 4 °C overnight. Antibodies were detected with horseradish peroxidase (HRP)-conjugated secondary antibody and developed with an enhanced chemiluminescence detection kit (Luminata Crescendo Western HRP Substrate, or Immobilon Western Chemiluminescent HRP Substrate, Millipore Corporation, Billerica, MA, USA). Membranes were tested for β-actin (Santa Cruz Biotechnology, Inc., Santa Cruz, CA, USA) to confirm equal loading.

ELISA Analysis. After serum was acquired as above, ELISA analysis was proceeded according to the protocol of human pigment epithelium-derived factor (PEDF) ELISA KIT (R&D Systems, Minneapolis, MN, USA). In brief, samples were added into a monoclonal antibody (McAb)-coated pore plate to incubate for 30 min at 37 °C. After washed for 5 times, enzyme standard reagent was added for 50 μL per well following incubated and washed. After added A solution, B solution and stop buffer in turn, samples were measured with MTT assay at 450-nm wavelength.

Safety Evaluation. *Body Weight, Continuously Observation and HE Staining.* To estimate the potential side effects in the FLP/PEDF-treated mice, they were continuously observed for appearance, weight, independent activity and toxic deaths. The body weights were measured and recorded once three days. Vital organs (heart, liver, spleen, lung and kidney) were collected after sacrifice for HE staining and observed by two pathologists in a blinded manner.

Serological and Biochemical Analysis. Whole blood, obtained from mice, was divided into two parts. One was directly used to conduct a whole blood analysis using a Celltac alpha MEK-6318K fully automatic hematology analyzer (Nihon Kohden Corp., Shinjuku-ku, Tokyo, Japan) and the other was processed with EDTA-2K for 2–3 h at room temperature and serum was obtained by centrifugation.

Statistical Analysis. Statistic analysis was performed using One-Way ANOVA in Statistical Product and Service Solutions (SPSS V 19.0, IBM Corp., New York, USA). When equal variances were assumed after homogeneity of variance test, the Tukey multiple comparisons test was used. When equal variances were not assumed after homogeneity of variance test, Tamhane's T2 multiple comparisons test was used. Differences were considered statistically significant at $p < 0.05$.

Results and Discussions

Synthesis and Characterization of F-PEG-Chol. The ¹H-NMR spectra was the same as the previous paper²⁶, which proved that F-PEG-Chol was successfully synthesized by the modified two-step reaction. Due to the optimized synthetic process parameters, the purification of the intermediate H₂N-PEG-Chol became dramatically simpler than before²⁵, thereby improving the efficiency and yield.

Preparation and Characterization of FLP/PEDF. FLP was successfully prepared by a simple self-assembly method. As shown in Fig. 2A,B, the mean particle size of FLP was about 80 nm with a narrow polydispersity index (PDI) and the zeta-potential of FLP was around 35 mV. After incubation with PEDF gene to form FLP/PEDF, the diameter increased to about 200 nm while the zeta-potential decreased to around 20 mV due to the electrostatic interaction between gene and cationic nano-liposomes. When plasmid DNA with a negative charge bound with liposomes, the positive charge of liposomes was neutralized, which led to a decrease in the positive charge of the formed lipoplex. Besides, the sizes of lipoplexes increased mainly resulted from the plasmid DNA incubated on the surface to form a hydration shell. PLP and PLP/PEDF also had similar results in the diameter and zeta-potential. Figure 2C displayed the morphological characteristic of FLP/PEDF by TEM as

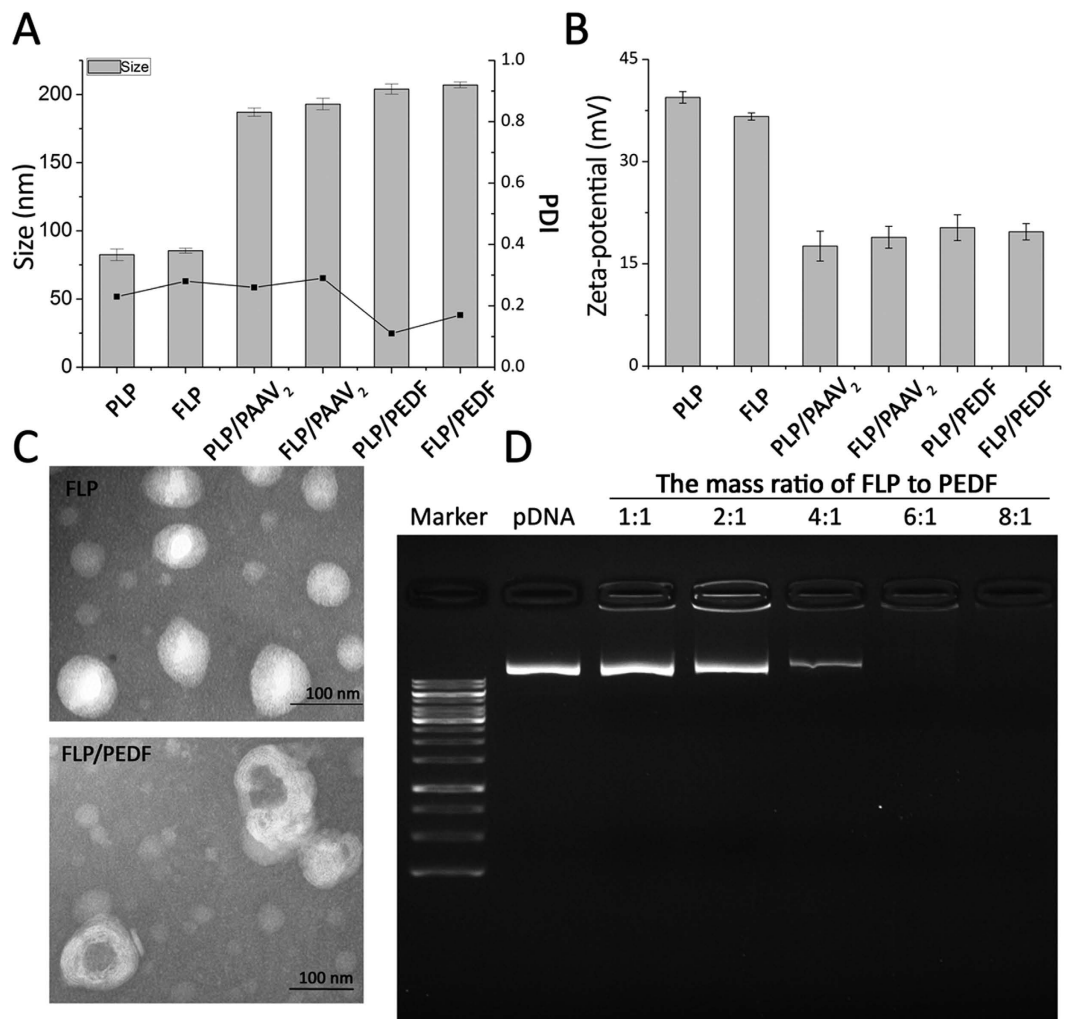


Figure 2. Pharmaceutical characteristics of FLP/PEDF by comparable study. (A) Mean diameters and polydispersity index (PDI) of nano-liposomes and nano-lipplexes. Mean \pm SD, $n = 3$. (B) Zeta-potentials of nano-liposomes and nano-lipplexes. Mean \pm SD, $n = 3$. (C) Morphological profiles of FLP and FLP/PEDF by transmission electron microscope (TEM). (D) Agarose gel electrophoresis was used to test the gene loading capacity of FLP. When the mass ratio of FLP to PEDF gene was up to 6:1, PEDF gene was completely encapsulated into FLP.

compared to FLP. FLP/PEDF, presenting a typical lipid-membrane structure with spherical outline, conforming to the measurement by dynamic light scattering.

Agarose gel electrophoresis could analyze the gene loading of FLP because the free PEDF gene un-entrapped into nano-liposomes could be detected and shown as a bright band with the same electrophoresis mobility shift as pDNA. As presented in Fig. 2D, the free PEDF gene decreased as the FLP amount increased. When the mass ratio of FLP to PEDF gene was up to 6:1, PEDF gene was completely encapsulated into FLP, which means if the mass ratio was no less than 6:1, PEDF could be encapsulated into FLP completely such as 8:1 and even higher. It could be inferred that FLP were one of promising vectors with high capacity for PEDF gene delivery.

HeLa cells Overexpressed FR α . The receptor detection assay demonstrated that 99.43% HeLa cells expressed FR α (Fig. 3A), indicating that HeLa cells we obtained were suitable model cells to investigate the targeting therapeutic effect of FLP/PEDF mediated by FR α .

FLP Transfected HeLa cells with High Efficiency. The pGFP, a tool gene, was selected to assess the transfection efficiency of FLP. As seen in Fig. 3B,C, GFP achieved the most efficient expression in HeLa cells treated by FLP/GFP among the four groups. The transfection efficiency of FLP/GFP was significantly higher than PLP/GFP ($p < 0.001$), illustrating that the cells had enhanced uptake of FLP/GFP by their FR α . PEGylation is thought to decline the cell uptake efficiency³¹. Actually, PLP/GFP presented lower transfection ability than LP/GFP in this study ($p < 0.001$). However, FLP/GFP make the negative effect of PEGylation negligible through introduction of folate ligand. Lipo2000 is one of commercial transfection reagents used widely because of its high transfection efficiency^{32,33}. FLP/GFP exhibited higher transfection efficiency than Lipo2000 in HeLa cells ($p < 0.001$), indicating that FLP were potential gene vectors for cervix cancer therapy.

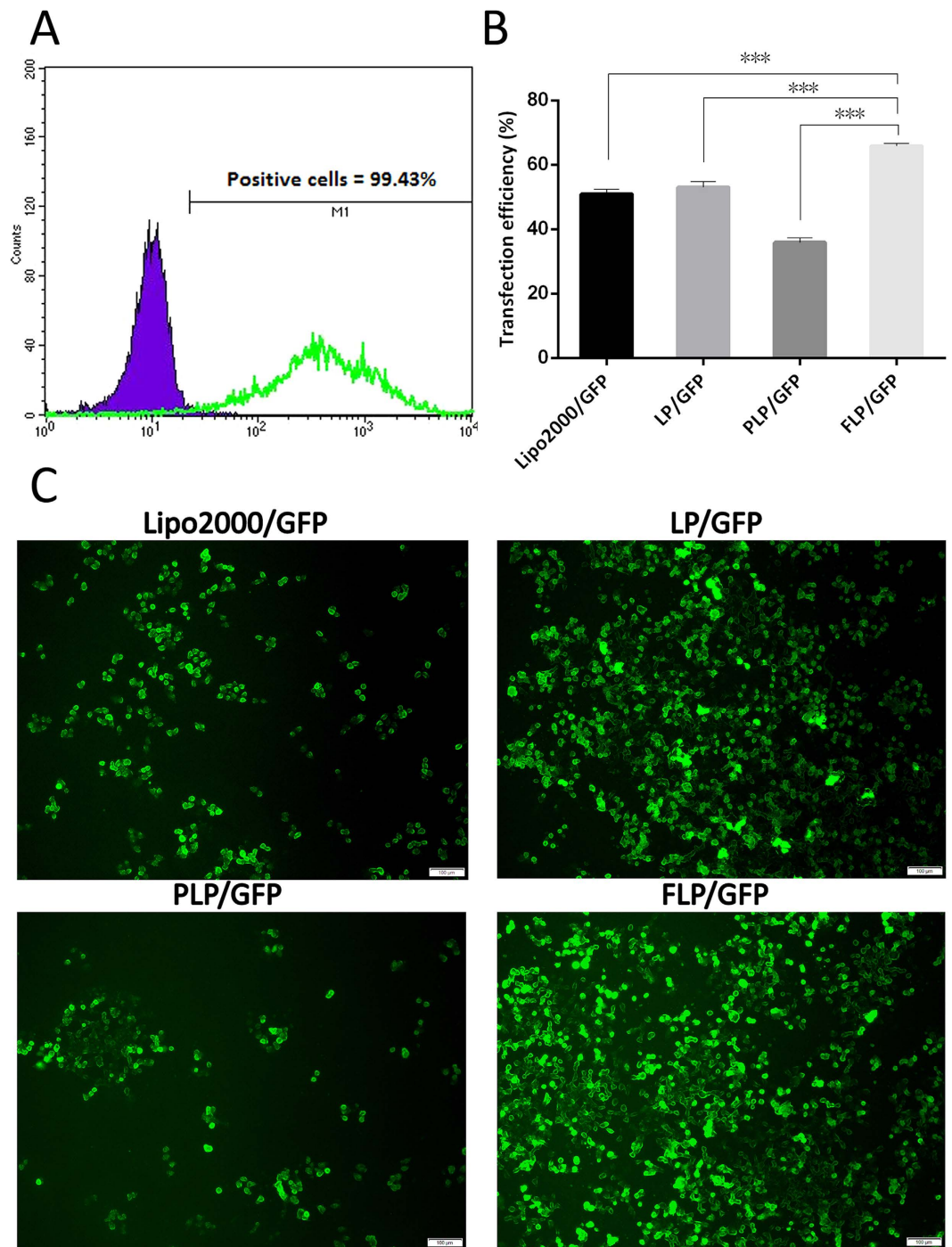


Figure 3. Detection of FR α expressed on human cervical cancer cells (HeLa cells) and transfection assessment of FLP/GFP in HeLa cells. (A) 99.43% of HeLa cells express FR α . (B) Transfection efficiency was measured by flow cytometer in nano-lipoplexes treated cells. FLP achieved the most efficient expression of GFP (green fluorescent stains). Mean \pm SD, $n = 3$, *** $p < 0.001$. (C) The representative images of transfected HeLa cells by inverted fluorescence microscope.

FLP/PEDF Inhibited the Growth of HeLa Cells and HUVEC Cells *in vitro*. The cytotoxicity of FLP/PEDF on HeLa cells and HUVEC cells was investigated using FLP/PAAV₂ and PLP/PEDF as the main contrast agents. The results demonstrated that the growth inhibition effects of FLP/PEDF on HeLa cells and HUVEC cells were concentration-dependent and time-dependent (Fig. 4A). FLP/PAAV₂ were cytotoxic to HeLa cells, probably because of the positive surface charge³⁴. FLP/PEDF inhibited the growth of HeLa cells more efficiently than FLP/PAAV₂, implicating the expressing PEDF had better *in vitro* activity. More strongly cytotoxic effects of FLP/PEDF on HeLa cells were found when compared to PLP/PEDF, which might be attributed to the enhanced expression of PEDF mediated by FR α expressed in HeLa cells. We previously reported that PLGA nanoparticles

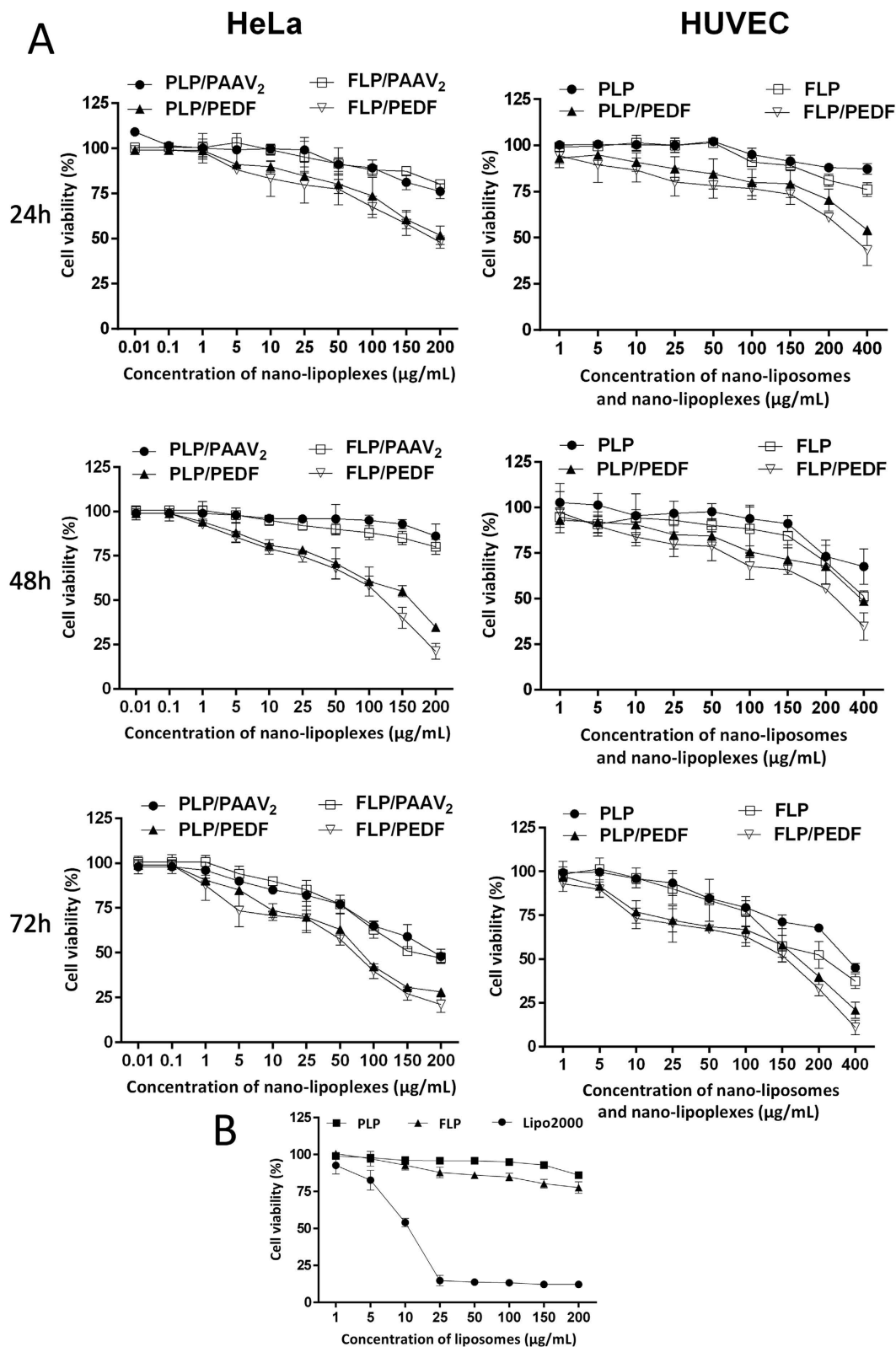


Figure 4. The cytotoxic study by MTT assay. Mean \pm SD, $n = 3$. (A) The toxicity of different nano-lipoplexes on HeLa cells and the growth inhibition effect of nano-liposomes and nano-lipoplexes on human umbilical vein endothelial cells (HUVEC Cells) after co-culture for 24 h, 48 h and 72 h, which were concentration-dependent and time-dependent. (B) The toxicity of Lipo2000, PLP and FLP on HeLa cells after 48 h of treatment.

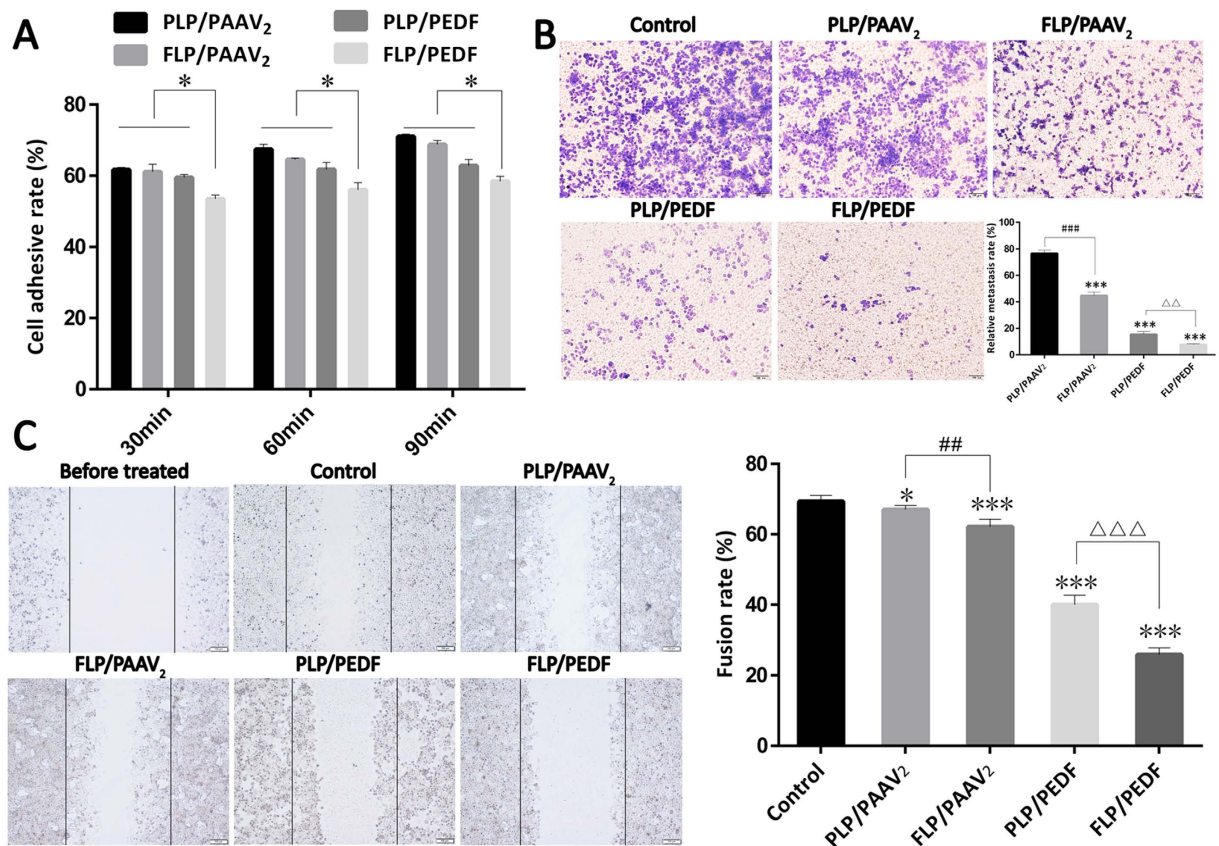


Figure 5. *In vitro* anti-metastasis research of FLP/PEDF. Mean \pm SD, $n = 3$. (A) Adhesion assay. FLP/PEDF significantly decreased HeLa cells adhesive rate at all the determined time points compared to control, PLP/PEDF, FLP/PAAV₂ and PLP/PAAV₂. * $p < 0.05$. (B) Representative images of migrated HeLa cells derived from invasion assay and relative metastasis rates of HeLa cells. FLP/PEDF observably restrain HeLa cells invasion. *** $p < 0.001$, all the nano-lipoplexes versus control. $\Delta\Delta p < 0.01$. ### $p < 0.001$. (C) Representative images of scratch assay and fusion rates of HeLa cells. * $p < 0.05$, PLP/PAAV₂ versus control. *** $p < 0.001$, the other three nano-lipoplexes versus control. ## $p < 0.01$. $\Delta\Delta\Delta p < 0.001$.

loaded with PEDF gene could dramatically inhibit HUVEC cells growth and antiangiogenesis^{16,17}. FLP/PEDF developed in this study also had similar effect. Lipo2000 only has limited application due to its toxicity. FLP had markedly lower cytotoxicity than Lipo2000 (Fig. 4B) probably because of the reduced zeta potential ascribing to PEGylation. All the data indicated that FLP with low toxicity was suitable to carry PEDF and FLP/PEDF might have the potential to inhibit the tumor growth and partly angiogenesis *in vitro*.

FLP/PEDF Inhibited Adhesion, Invasion and Migration of HeLa cells *in vitro*. PEDF has been reported to play an important role on the metastasis of tumor cells^{35,36}. It could suppress lung and bone metastasis of osteosarcoma³⁷, reducing the transfer of melanoma to lung and liver³⁸. Therefore, the effect of FLP/PEDF on HeLa cells metastasis *in vitro* was investigated through the adhesion, invasion and migration assay. As shown in Fig. 5A, the adhesion rate of HeLa cells rose over time in all the four groups treated by nano-lipoplexes, among which cells transfected by FLP/PEDF had the lowest adhesion rate at all the determined time points ($p < 0.05$). FLP/PEDF reduced the adhesion of HeLa cells more significantly than PLP/PEDF, probably attributing to the enhanced expression of PEDF. The invasion and scratch assay also revealed the similar trend among the four nano-lipoplexes: FLP/PEDF presented the strongest inhibition of HeLa cells invasion and the lowest cell fusion rate (Fig. 5B,C, respectively). According to the data, it could be inferred that FLP/PEDF could inhibit the metastasis of HeLa cells by affecting their adhesion, invasion and migration.

FLP/PEDF Inhibited the Growth of Abdominal Metastatic Tumor from Cervical Cancer *in vivo*. The abdominal metastatic tumor model of cervical cancer was successfully established by injecting HeLa cells into the abdomen. The intraperitoneal injection for FLP/PEDF administration was selected in this study, which would achieve higher anti-tumor efficacy and be easy to bring about the clinic transformation. The therapeutic results displayed that FLP/PEDF could more efficiently diminish tumor nodules (Fig. 6A,B), decrease tumor weight (Fig. 6C) and reduce the formation of relative ascites (Fig. 6D) than all the contrast preparations. The folate ligand in FLP/PEDF might selectively deliver the nano-lipoplexes to HeLa cells by the specific recognition of FR α having high affinity with folic acid³⁹. Furthermore, the enhanced uptake of FLP/PEDF mediated by FR α probably contributed to the improvement of PEDF expression, hence leading to stronger anti-tumor activity than PLP/PEDF. Interestingly, the nano-lipoplexes

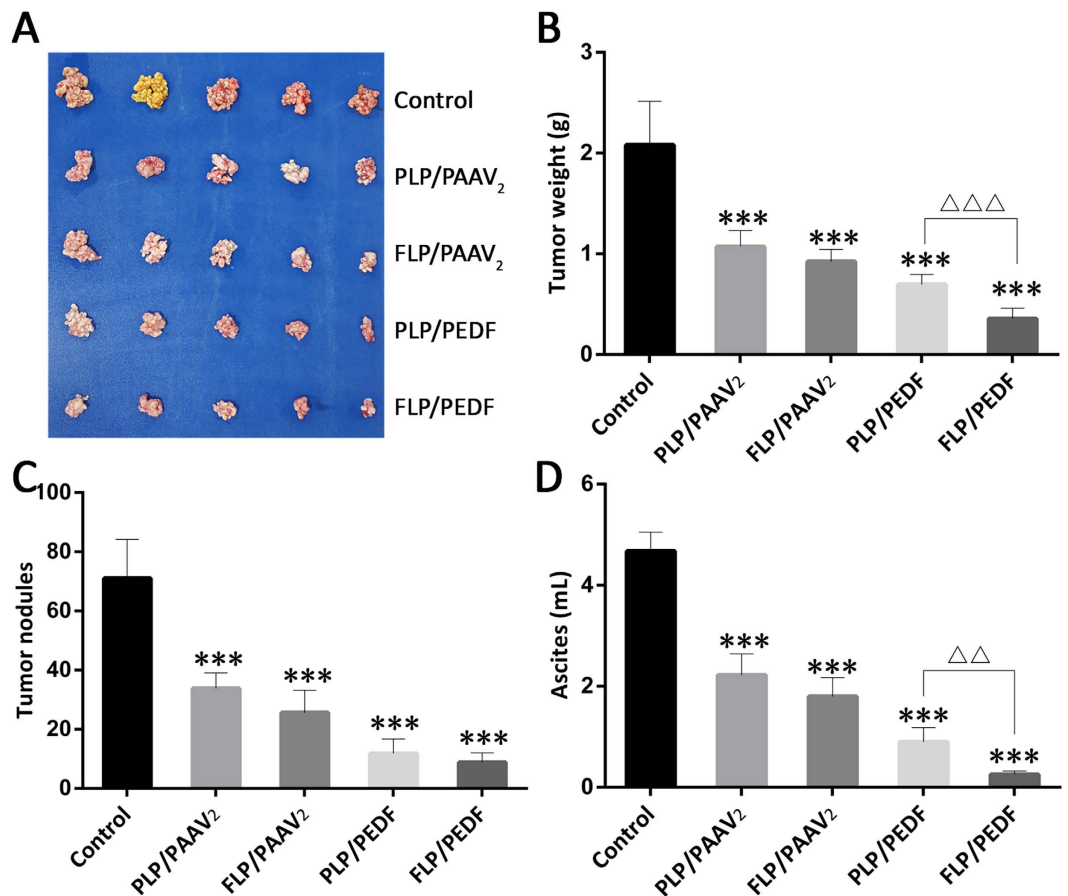


Figure 6. *In vivo* anti-tumor effect of FLP/PEDF by comparison with control, PLP/PAAV₂, FLP/PAAV₂, PLP/PEDF. The abdominal metastatic tumor model of cervical cancer was established by injecting HeLa cells into the abdomen, and these nude mice were treated by intraperitoneal injection. FLP/PEDF exhibited a superior anti-tumor effect. Mean \pm SD, n = 5. ***p < 0.001, all the nano-lipoplexes versus control. (A) Photographs of cervical tumor tissues. (B) Weight of tumors. $\Delta\Delta\Delta$ p < 0.001. (C) Amount of tumor nodules. (D) Volume of ascites. $\Delta\Delta$ p < 0.01.

encapsulating PAAV₂ including FLP/PAAV₂ and PLP/PAAV₂ also had tumor growth inhibition effect. This phenomenon might result from the cytotoxic effect of vectors with positive surface charge themselves and the related humoral immune reaction stimulated by the plasmid vector itself. Thus, FLP/PEDF with multiple effects could play more forceful anti-cancer effect on cervical cancer *in vivo* than single PEDF treatment¹³.

FLP/PEDF Up-regulated the PEDF Expression in Tumor Tissues and Serum. The PEDF level in cervix carcinoma was reported to be lower than that in normal cervical tissue⁴⁰. Introduction of exogenous PEDF could enhance the therapeutic efficacy of cervical cancer. IHC staining and western blot analysis were employed to detect the expression of PEDF. As shown in Fig. 7A,B, PEDF (brown stain) expressed in all tumor tissues from the five groups. Only extremely low PEDF expression was found in the control group, while a large amount of PEDF dispersed in the tumor tissue of FLP/PEDF treated group. FLP/PEDF resulted in a significant increase of near 100% in PEDF expression in HeLa cells *in vivo* as compared to PLP/PEDF (p < 0.001), which might be caused by the modification of folate ligand on the nano-lipoplexes as discussed above. The western blot result displayed in Fig. 7C further confirmed the data provided by IHC: FLP/PEDF indeed enhanced the PEDF expression dramatically in the abdominal metastatic tumor from cervical cancer. PEDF, a typical secretory protein, could excrete into blood except tissue distribution⁴¹. Thus, the ELISA analysis was carried out to determine the PEDF concentration in mice serum. As seen in Fig. 7D, all the tumor bearing mice had PEDF detected in serum. The serum PEDF slightly elevated after treated by PLP/PEDF (p < 0.05), while dramatically increased after treatment with FLP/PEDF. Taken together, FLP/PEDF could effectively transfect HeLa cells *in vivo* and successfully achieved PEDF expression with high efficiency, demonstrating that FLP were hopeful vectors for PEDF delivery specific to cervix cancer cells *in vivo* by intraperitoneal administration.

FLP/PEDF Suppressed Angiogenesis, Inhibited Cell Proliferation and Induced Cell Apoptosis *in vivo*. The potential mechanism underlying the anti-tumor efficacy of FLP/PEDF-based therapy was investigated by CD31 staining, Ki₆₇ staining and TUNEL assay. It had been reported that cervical cancer was angiogenesis-dependent³⁶. PEDF in an increasing level resulted in tumor suppression by inhibiting

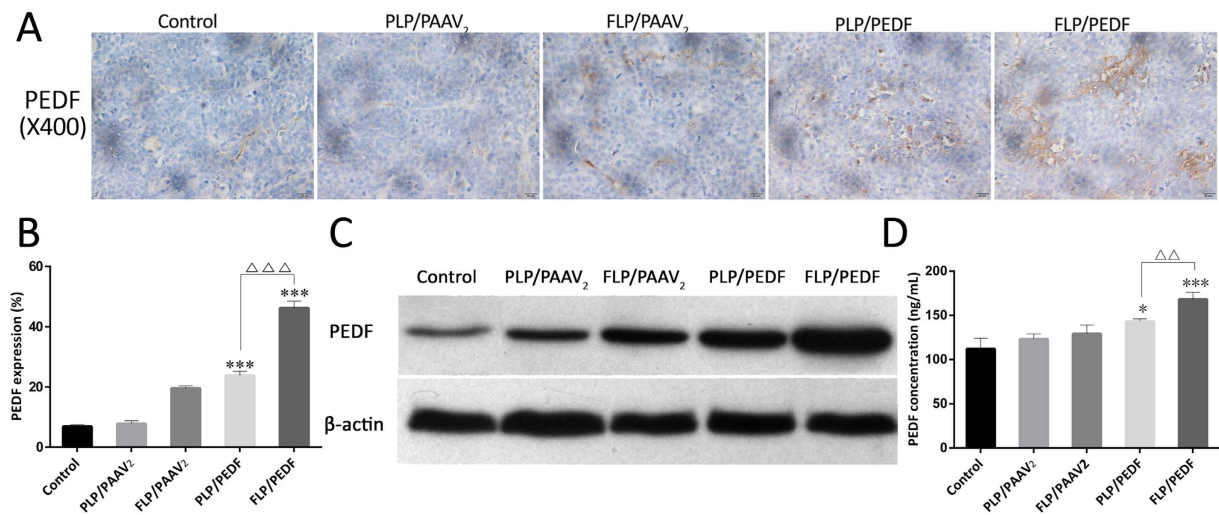


Figure 7. FLP/PEDF dramatically up-regulated the PEDF expression in tumor tissues and serum.

(A) Representative immunohistochemical image of PEDF (brown stains) expressed in tumor tissues in each group ($\times 200$). (B) Statistical results of PEDF in tumor tissues. $***p < 0.001$, FLP/PEDF and PLP/PEDF versus control. $\Delta\Delta\Delta p < 0.001$. (C) Semi-quantitative assay of PEDF expressed in tumor tissues by Western blot analysis. (D) Concentrations of PEDF secreted into serum by ELISA assay. $***p < 0.001$, FLP/PEDF versus control. $*p < 0.05$, PLP/PEDF versus control. $\Delta\Delta p < 0.01$.

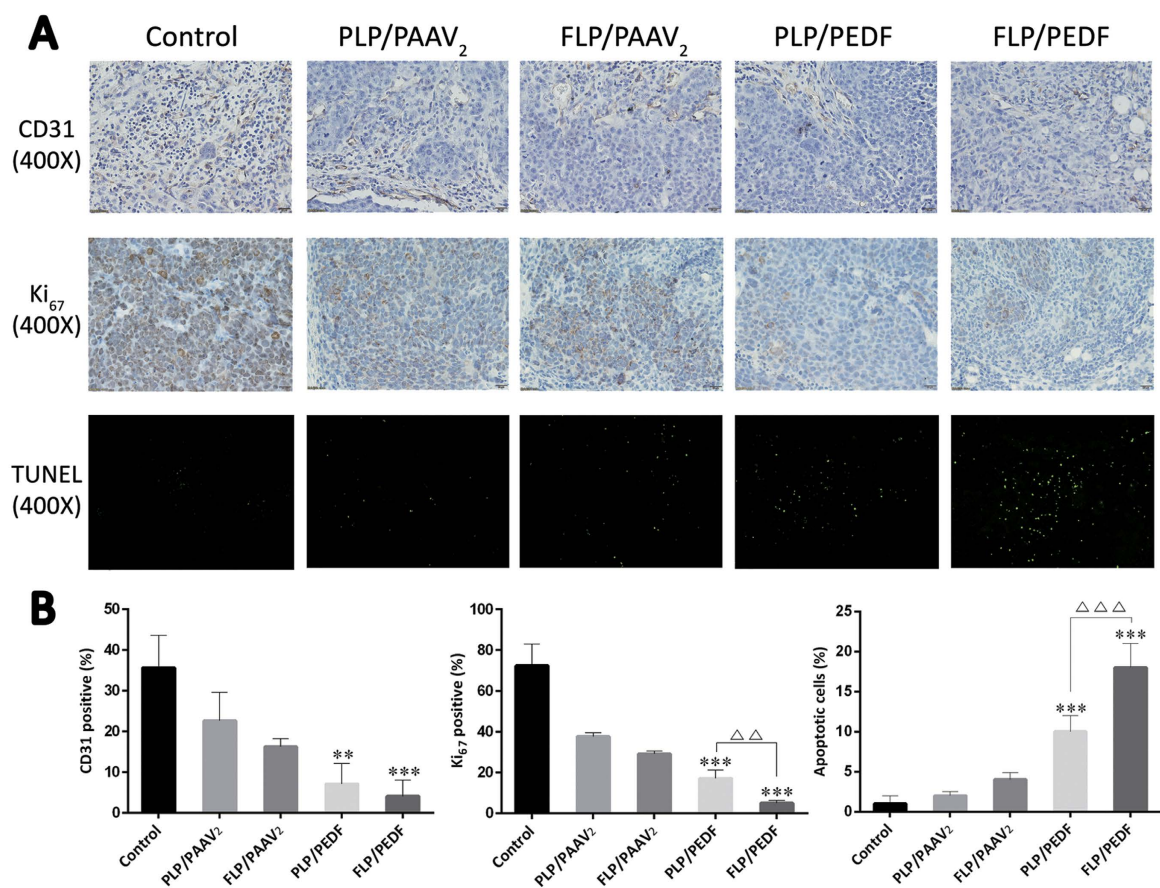


Figure 8. FLP/PEDF remarkably suppressed angiogenesis, inhibited cell proliferation and induced cell apoptosis *in vivo*. The microvessel density (MVD) was assessed by CD31 staining. The proliferative profile of HeLa cells *in vivo* was investigated through Ki₆₇ staining analysis. Moreover, TUNEL was employed to evaluate tumor cell apoptosis. (A) Representative immunohistochemical images of tumor sections in each group ($\times 400$). (B) Statistical results of MVD, proliferative cells and apoptotic cells. $**p < 0.01$, treated group versus control. $***p < 0.001$, treated group versus control. $\Delta\Delta p < 0.01$. $\Delta\Delta\Delta p < 0.001$.

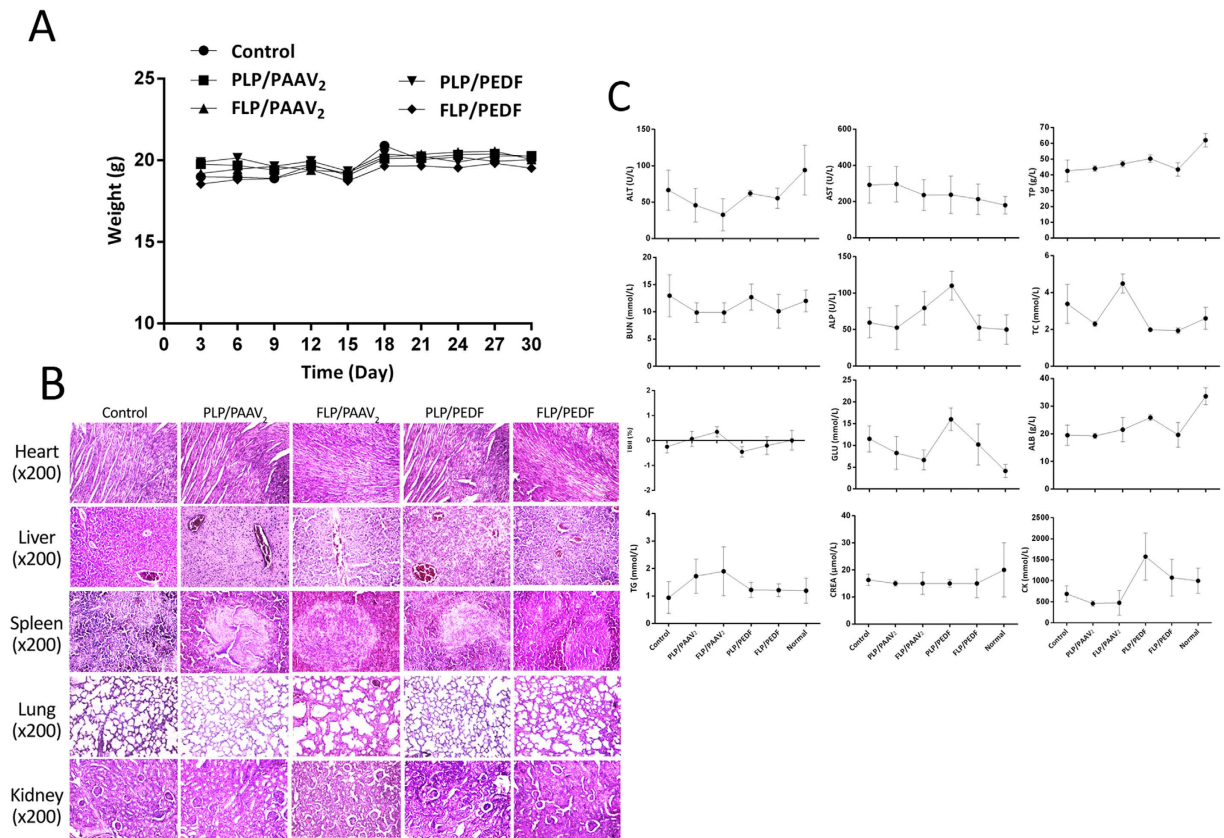


Figure 9. Preliminary safety evaluation of FLP/PEDF in female mice bearing tumor. Mean \pm SD, $n = 5$. (A) Body weight of tumor-bearing mice in each group. FLP/PEDF caused no weight change during treatment. (B) Serological and biochemical indexes determined at the therapeutic end point. FLP/PEDF treatment contributed to better AST, TC and CK levels approaching to the normal ranges. (C) Representative H&E images ($\times 200$) of vital organs including heart, liver, spleen, lung and kidney. FLP/PEDF had no obvious toxicity on these tissues.

neovascularization³⁷. The endothelial cells of tumor new blood vessels express CD31, which is often used to evaluate the degree of tumor angiogenesis and imply a rapidly growing tumor. Thus, CD31 expression was examined by IHC staining to study the effect of FLP/PEDF on angiogenesis in this study. As shown in Fig. 8A,B, FLP/PEDF sharply reduced CD31 positive cells (brown stains) to 5% and significantly decreased microvessel density (MVD) compared with PLP/PEDF and control ($p < 0.001$). This mainly ascribed to the improved expression of PEDF. PEDF was reported to suppress tumor cell proliferation¹³. The Ki₆₇ staining analysis (brown stains) in this study showed that FLP/PEDF treatment resulted in 10% of Ki₆₇ expression, whereas PLP/PEDF treatment resulted in 20% of Ki₆₇ expression. FLP/PEDF, with elevated PEDF expression, presented significantly efficient inhibition activity on the proliferation of HeLa cells *in vivo* than PLP/PEDF ($p < 0.01$). Furthermore, TUNEL was used to evaluate tumor cell apoptosis in the mice treated by the four nano-lipoplexes because it could detect DNA fragmentation derived from apoptotic signals. According to the green fluorescent spots, the tumor cell apoptosis was specifically increased (18-fold, versus control, $p < 0.001$) when the mice were treated by FLP/PEDF but only 10-fold after they were exposed to PLP/PEDF. Similar to the suppressive effect of tumor growth, FLP/PAAV₂ and PLP/PAAV₂ also slightly affected angiogenesis of tumor, proliferation and apoptosis of HeLa cells. Both nano-lipoplexes with positive zeta potentials might be cytotoxic to the endothelial cells in tumor tissue, which caused down-regulated neovascularization. Moreover, they were capable of inhibiting proliferation and promoting apoptosis *in vivo* which was similar to the cytotoxic effect *in vitro*. These results demonstrated that the highly efficient anti-tumor activity of FLP/PEDF might involve the suppression of angiogenesis, inhibition of cell proliferation and cell apoptosis by not only PEDF with enhanced expression but the vector itself.

FLP/PEDF were Relatively Non-toxic to Female Mice Bearing Tumor. PEDF was reported to have no tissue specificity³⁹, which might cause side effects on normal endothelial cells or some normal tissues. Our ELISA analysis also confirmed that PEDF indeed secreted into blood, although FLP/PEDF were administered by locally intraperitoneal injection. Thus, the preliminary safety evaluation of FLP/PEDF was performed in the female mice bearing tumor by body-weight monitoring during treatment, organs biopsy, serological and biochemical analysis at the therapeutic end point. In the whole process of animal experiments, the appearance of mice remained hairless and albino in background until they were sacrificed. Normal urine and fecal appearances were found during treatment in all the groups. Near the end of treatment, the nude mice were unable to move

freely because of malignancy-related ascites especially in control group but not in FLP/PEDF-treated one. The total body weight of FLP/PEDF-treated mice had no difference with those treated by other nano-lipoplexes or control (Fig. 9A). HE staining presented no significantly toxic pathological changes in the heart, liver, spleen, lung and kidney derived from FLP/PEDF-treated mice as shown in Fig. 9B. Moreover, all the biochemical indexes illustrated that the vital organs' functions of FLP/PEDF-treated mice were present at the similar levels according to the data of normal mice (Fig. 9C), among which AST, TC and CK were approaching to the normal ranges. It could be inferred that FLP/PEDF were one of relatively safe formulations by intraperitoneal administration for the treatment of female mice bearing tumor probably because the increased PEDF in blood is not enough to induce toxic effects.

Conclusion

The targeting lipid F-PEG-Chol was expectably synthesized by a novel method, and FR α -targeted nano-lipoplexes loaded with PEDF gene (FLP/PEDF) were successfully developed by a film dispersion method for the first time. The cervical cancer therapeutic effects were systemically investigated *in vitro* and *in vivo*. FLP/PEDF could efficiently transfect HeLa cells, inhibit the growth of HeLa cells and HUVEC cells, suppress adhesion, invasion and migration of HeLa cells *in vitro*. Moreover, FLP/PEDF exhibited a superior anti-tumor effect than non-targeting nano-lipoplexes, possibly due to selective delivery of PEDF to HeLa cells involving the over-expressing FR α with specific recognition of folate ligand. FLP/PEDF play forceful effect on cervical cancer treatment by not only PEDF at an elevating level but the vector itself (involving the nano-liposomes with positive surface charge and plasmid vector). The deep study of the mechanism demonstrated that the highly efficient anti-tumor activity of FLP/PEDF was related to the suppression of angiogenesis, inhibition of cell proliferation and cell apoptosis. The preliminary safety evaluation confirmed that FLP/PEDF by intraperitoneal administration were relatively safe. In sum, FLP were promising carriers for PEDF gene and FLP/PEDF were potential for future cervical cancer gene therapy.

References

1. Siegel, R. L., Miller, K. D. & Jemal, A. Cancer Statistics, 2015. *CA-Cancer J. Clin.* **65**, 5–29 (2015).
2. Blomfield, P. Management of Cervical Cancer. *Aust. Fam. Physician* **36**, 122 (2007).
3. Petignat, P. & Roy, M. Diagnosis and Management of Cervical Cancer. *Brit. Med. J.* **335**, 765 (2007).
4. Michael, E. Gene Types Transferred in Gene Therapy Clinical Trials. *J. Gene Med.* Date of access: 7/2015 (2015).
5. Becerra, S. P. Focus on Molecules: Pigment Epithelium-Derived Factor (PEDF). *Exp. Eye Res.* **82**, 739–740 (2006).
6. Yang, H. & Grossniklaus, H. E. Constitutive Overexpression of Pigment Epithelium-Derived Factor Inhibition of Ocular Melanoma Growth and Metastasis. *Invest. Ophthalm. Vis. Sci.* **51**, 28–34 (2010).
7. Ek, E. T., Dass, C. R. & Choong, P. F. PEDF: A Potential Molecular Therapeutic Target with Multiple Anti-Cancer Activities. *Trends Mol. Med.* **12**, 497–502 (2006).
8. Quan, G. & Choong, P. F. Anti-Angiogenic Therapy for Osteosarcoma. *Cancer Metast. Rev.* **25**, 707–713 (2006).
9. Chen, J., Ye, L., Zhang, L. & Jiang, W. The Molecular Impact of Pigment Epithelium-Derived Factor, PEDF, on Lung Cancer Cells and the Clinical Significance. *Int. J. Oncol.* **35**, 159–166 (2009).
10. Cai, J., Parr, C., Watkins, G., Jiang, W. & Boulton, M. Decreased Pigment Epithelium-Derived Factor Expression in Human Breast Cancer Progression. *Clin. Cancer Res.* **12**, 3510–3517 (2006).
11. Filleur, S. *et al.* Two Functional Epitopes of Pigment Epithelial-Derived Factor Block Angiogenesis and Induce Differentiation in Prostate Cancer. *Cancer Res.* **65**, 5144–5152 (2005).
12. Cheung, L. *et al.* Pigment Epithelium-Derived Factor is Estrogen Sensitive and Inhibits the Growth of Human Ovarian Cancer and Ovarian Surface Epithelial Cells. *Endocrinology* **147**, 4179–4191 (2006).
13. Yang, J. *et al.* Growth Suppression of Cervical Carcinoma by Pigment Epithelium-Derived Factor via Anti-Angiogenesis. *Cancer Biol. Ther.* **9**, 967–974 (2010).
14. Chen, Q. *et al.* Antitumor Activity of Placenta-Derived Mesenchymal Stem Cells Producing Pigment Epithelium-Derived Factor in a Mouse Melanoma Model. *Oncol. Lett.* **4**, 413–418 (2012).
15. Gao, Y. *et al.* Human Mesenchymal Stem Cells Overexpressing Pigment Epithelium-Derived Factor Inhibit Hepatocellular Carcinoma in Nude Mice. *Oncogene* **29**, 2784–2794 (2010).
16. Cui, F. *et al.* The Pigment Epithelial-Derived Factor Gene Loaded in PLGA Nanoparticles for Therapy of Colon Carcinoma. *Oncol. Rep.* **24**, 661–668 (2010).
17. Yu, T. *et al.* Pigment Epithelial-Derived Factor Gene Loaded Novel CPPC Nanoparticles Promoted Tumor Suppression by Systemic Administration. *Int. J. Nanomed.* **11**, 743–759 (2016).
18. Xu, B. *et al.* Polymeric Nanomedicine for Combined Gene/Chemo-Therapy Elicits Enhanced Tumor Suppression. *Mol. Pharm.* **13**, 663–676 (2016).
19. Gong, C. & F. Y. Research Progress of the Folate Receptor in Cervical Cancer. *China Medical Herald* **11**, 164–167 (2014).
20. You, H. *et al.* Study of the Synergistic Effect of Folate-Decorated Polymeric Micelles Incorporating Hydroxycamptothecin with Radiotherapy on Xenografted Human Cervical Carcinoma. *Colloid. Surface. B.* **140**, 150–160 (2016).
21. Prasad, R., Aiyer, S., Chauhan, D. S., Srivastava, R. & Selvaraj, K. Bioresponsive Carbon Nano-Gated Multifunctional Mesoporous Silica for Cancer Theranostics. *Nanoscale* **8**, 4537–4546 (2016).
22. He, Z. *et al.* Folate-Linked Lipoplexes for Short Hairpin RNA Targeting Claudin-3 Delivery in Ovarian Cancer Xenografts. *J. Control. Release* **172**, 679–689 (2013).
23. He, Z. *et al.* Development of Glycyrrhetic Acid-Modified Stealth Cationic Liposomes for Gene Delivery. *Int. J. Pharm.* **397**, 147–154 (2010).
24. Li, J. *et al.* Micelles Based on Methoxy Poly (Ethylene Glycol) Cholesterol Conjugate for Controlled and Targeted Drug Delivery of a Poorly Water Soluble Drug. *J. Biomed. Nanotechnol.* **8**, 809–817 (2012).
25. He, Z. *et al.* Gene Delivery with Active Targeting to Ovarian Cancer Cells Mediated by Folate Receptor α . *J. Biomed. Nanotechnol.* **9**, 833–844 (2013).
26. Xiang, G., Wu, J., Lu, Y., Liu, Z. & Lee, R. J. Synthesis and Evaluation of a Novel Ligand for Folate-Mediated Targeting Liposomes. *Int. J. Pharm.* **356**, 29–36 (2008).
27. Song, X. *et al.* Development of PLGA Nanoparticles Simultaneously Loaded with Vincristine and Verapamil for Treatment of Hepatocellular Carcinoma. *J. Pharm. Sci.* **99**, 4874–4879 (2010).
28. Yu, J. *et al.* Arsenic Trioxide (As₂O₃) Reduces the Invasive and Metastatic Properties of Cervical Cancer Cells *in vitro* and *in Vivo*. *Gynecol. Oncol.* **106**, 400–406 (2007).

29. Chu, Y. *et al.* MicroRNA-590 Promotes Cervical Cancer Cell Growth and Invasion by Targeting CHL1. *J. Cell. Biochem.* **115**, 847–853 (2014).
30. Peng, Y. *et al.* Effects and Mechanism of Baicalin on apoptosis of Cervical Cancer HeLa *in-Vitro*. *Iran. J. Pharm. Res.* **14**, 251–261 (2015).
31. Stefanick, J. F., Ashley, J. D., Kiziltepe, T. & Bilgicer, B. A Systematic Analysis of Peptide Linker Length and Liposomal Polyethylene Glycol Coating on Cellular Uptake of Peptide-Targeted Liposomes. *ACS nano* **7**, 2935–2947 (2013).
32. Vulugundam, G., Kumar, K., Kondaiah, P. & Bhattacharya, Santanu Efficacious Redox-Responsive Gene Delivery in Serum by Ferrocenylated Monomeric and Dimeric Cationic Cholesterols. *Org. Biomol. Chem.* **13**, 4310–4320 (2015).
33. Chang, H., Tian, Y., Wang, J., Jie, X. & Gou, X. Effect of Specific TPX2-Sirna on Growth of Human Cervical Adenocarcinoma HeLa *in vitro*. *Chinese Journal of Clinical Oncology* **39**, 80–84 (2012).
34. Han, X. *et al.* 9-NC-Loaded Folate-Conjugated Polymer Micelles as Tumor Targeted Drug Delivery System: Preparation and Evaluation *in vitro*. *Int. J. Pharm.* **372**, 125–131 (2009).
35. Fitzgerald, D. P. *et al.* Opposing Effects of Pigment Epithelium-Derived Factor on Breast Cancer Cell Versus Neuronal Survival: Implication for Brain Metastasis and Metastasis-Induced Brain Damage. *Cancer Res.* **72**, 144–153 (2012).
36. Guan, M. *et al.* Adenovirus-mediated PEDF Expression Inhibits Prostate Cancer Cell Growth and Results in Augmented Expression of PAI-2. *Cancer Biol. Ther.* **6**, 419–425 (2007).
37. Dass, C. R., Contreras, K. G., Dunstan, D. E. & Choong, P. Chitosan Microparticles Encapsulating PEDF Plasmid Demonstrate Efficacy in an Orthotopic Metastatic Model of Osteosarcoma. *Biomaterials* **28**, 3026–3033 (2007).
38. Garcia, M. *et al.* Inhibition of Xenografted Human Melanoma Growth and Prevention of Metastasis Development by Dual Antiangiogenic/Antitumor Activities of Pigment Epithelial-Derived Factor. *Cancer Res.* **64**, 5632–5642 (2004).
39. Leamon, C. P. & Low, P. S. Folate-Mediated Targeting: from Diagnostics to Drug and Gene Delivery. *Drug Discov. Today* **6**, 44–51 (2001).
40. Liu, J., Cui, B., Yin, T. & Zhang, A. Expression and Significance of Pigment Epithelium-Derived Factor in Cervix Squamous Cell Carcinoma. *Journal of Shandong University (Health Sciences)* **50**, 103–106 (2005).
41. Yang, L. *et al.* Anti-Tumor Effect of Adenovirus-Mediated Gene Transfer of Pigment Epithelium-Derived Factor on Mouse B16-F10 Melanoma. *J. Exp. Clin. Onc. Res.* **28**, 1–11 (2009).

Acknowledgements

This work was financially supported by the National Natural Science Foundation of China (No. 81302729) and the Postdoctoral Science Foundation of China (No. 2014M562330).

Author Contributions

C.J., A.T. and X.S. contributed to the conception of the study. L.H., Y.L., S.X., A.F. and X.T. contributed to the funds of the study. Y.Y. contributed significantly to analysis and manuscript preparation. Y.Y. and Y.X. performed the data analyses and wrote the manuscript. Y.Y., Y.X., L.G. and Z.H. helped perform the analysis with constructive discussions.

Additional Information

Competing financial interests: The authors declare no competing financial interests.

How to cite this article: Yang, Y. *et al.* Promising Nanocarriers for PEDF Gene Targeting Delivery to Cervical Cancer Cells Mediated by the Over-expressing FR α . *Sci. Rep.* **6**, 32427; doi: 10.1038/srep32427 (2016).



This work is licensed under a Creative Commons Attribution 4.0 International License. The images or other third party material in this article are included in the article's Creative Commons license, unless indicated otherwise in the credit line; if the material is not included under the Creative Commons license, users will need to obtain permission from the license holder to reproduce the material. To view a copy of this license, visit <http://creativecommons.org/licenses/by/4.0/>

© The Author(s) 2016